

# Of Mice and Dogs: Species-Specific Differences in the Inflammatory Response Following Myocardial Infarction

Oliver Dewald, Guofeng Ren, Georg D. Duerr, Martin Zoerlein, Christina Klemm, Christine Gersch, Sophia Tinney, Lloyd H. Michael, Mark L. Entman, and Nikolaos G. Frangogiannis

*From the Section of Cardiovascular Sciences, Baylor College of Medicine, the Methodist Hospital, and the DeBakey Heart Center, Houston, Texas*

**Large animal models have provided much of the descriptive data regarding the cellular and molecular events in myocardial infarction and repair. The availability of genetically altered mice may provide a valuable tool for specific cellular and molecular dissection of these processes. In this report we compare closed chest models of canine and mouse infarction/reperfusion qualitatively and quantitatively for temporal, cellular, and spatial differences. Much like the canine model, reperfused mouse hearts are associated with marked induction of endothelial adhesion molecules, cytokines, and chemokines. Reperfused mouse infarcts show accelerated replacement of cardiomyocytes by granulation tissue leading to a thin mature scar at 14 days, when the canine infarction is still cellular and evolving. Infarcted mouse hearts demonstrate a robust but transient postreperfusion inflammatory reaction, associated with a rapid up-regulation of interleukin-10 and transforming growth factor- $\beta$ . Unlike canine infarcts, infarcted mouse hearts show only transient macrophage infiltration and no significant mast cell accumulation. In correlation, the growth factor for macrophages, M-CSF, shows modest and transient up-regulation in the early days of reperfusion; and the obligate growth factor for mast cells, stem cell factor, SCF, is not induced. In summary, the postinfarction inflammatory response and resultant repair in the mouse heart shares many common characteristics with large mammalian species, but has distinct temporal and qualitative features. These important species-specific differences should be considered when interpreting findings derived from studies using genetically altered mice. (*Am J Pathol* 2004, 164:665–677)**

For almost a century, experimental models of myocardial infarction have contributed to our understanding of the pathobiology of myocardial infarction. Large animal models have been extensively used to study the mechanisms involved in myocardial injury and repair<sup>1,2</sup> and have significantly contributed to our understanding of the pathological process of myocardial infarction. However, large animal studies have significant limitations in investigating the functional role of specific genes in myocardial ischemia. Recent advances in transgenic and gene targeting approaches have allowed sophisticated manipulations of genes whose functions may be important in injury and repair following myocardial infarction.<sup>3</sup> Because of technical and economic considerations, these experiments are largely confined to the mouse.<sup>4,5</sup> To capitalize on these advances in gene targeting technology murine models of experimental myocardial infarction have been developed<sup>6,7</sup> and have been extensively used to dissect the mechanisms involved in ischemic myocardial injury.<sup>8–10</sup> However, extrapolation of the findings derived from murine experiments to the human pathobiology requires similar disease mechanisms in both species. Despite the widespread use of murine models of myocardial infarction, detailed studies of the cellular and molecular events associated with repair of the mouse infarction are lacking.

This study examines the pathological features of myocardial infarction in mice, and compares the sequence of cellular and molecular events noted following murine coronary occlusion and reperfusion with the characteristics of reperfused infarcts in an established canine model. Both canine and murine infarcts exhibit a robust inflammatory response associated with induction of chemokines, cytokines and adhesion molecules. In comparison with higher mammals, mice show a more rapid and transient response and do not demonstrate up-regulation of growth factors supporting sustained survival of inflammatory leukocytes.

---

Supported by National Institutes of Health grant HL-42550, a grant from the American Heart Association, Texas affiliate, the DeBakey Heart Center, the Curtis Hankamer Research Fund, and the Deutsche Forschungsgemeinschaft (DE 801/1–1).

Accepted for publication November 3, 2003.

Address reprint requests to Nikolaos G. Frangogiannis, Section of Cardiovascular Sciences, One Baylor Plaza, M/S F-602, Baylor College of Medicine, Houston, TX 77030. E-mail: ngf@bcm.tmc.edu.

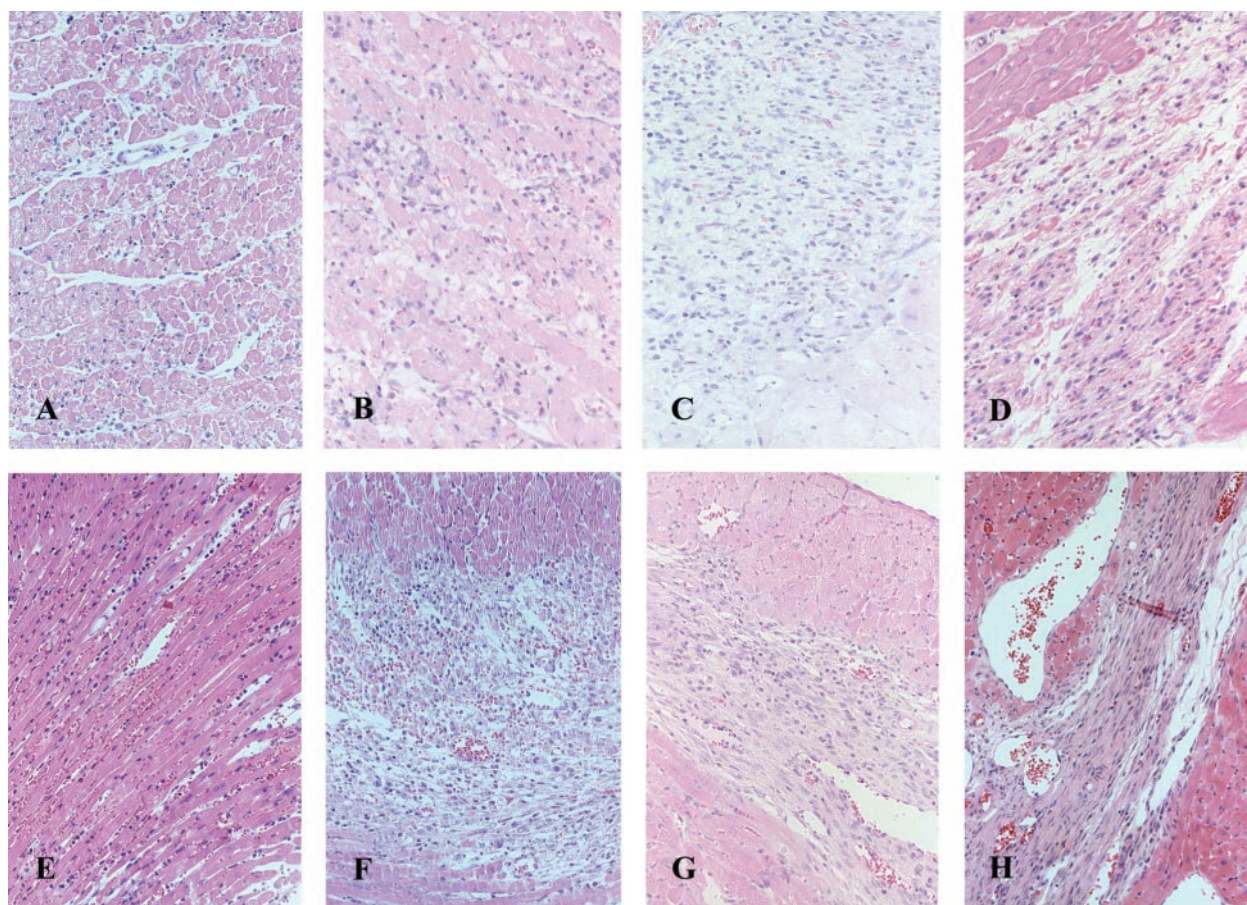


**Figure 1.** Progression of the healing process in reperfused canine (A–D) and murine (E–H) myocardial infarcts. Both canine (A) and murine (E) infarcts exhibit marked leukocyte infiltration after 24 hours of reperfusion. After 72 hours of reperfusion, dog infarcts show interstitial infiltration with inflammatory cells and fibroblasts (B) without significant cardiomyocyte replacement. In contrast, at the same time point, mouse infarcts show extensive cardiomyocyte replacement with granulation tissue (F). After 7 days of reperfusion the canine infarct is a highly cellular environment, whereas mouse infarcts exhibit areas of thinning. After 14 days of reperfusion the canine infarct still has a high cellular content (D). In contrast, the murine infarct shows thinned areas and large vascular structures (H). All sections are stained with hematoxylin and eosin (magnification,  $\times 100$ ).

## Materials and Methods

### Ischemia-Reperfusion Protocols

#### Murine Model

Male and female wild-type C57BL/6 mice (Harlan Sprague-Dawley, Houston, TX), 8 to 12 weeks of age (18.0–22.0 g body weight) were anesthetized by an intraperitoneal injection of sodium pentobarbital (60  $\mu\text{g/g}$ ). A closed-chest mouse model of myocardial ischemia-reperfusion was used as previously described,<sup>7</sup> to avoid the confounding effects of surgical trauma and inflammation, which may influence the baseline levels of chemokines and cytokines. Briefly, after thoracotomy, the pericardium was dissected and an 8–0 Prolene suture (Ethicon, Somerville, NJ) with the U-shaped tapered needle was passed under the left anterior descending (LAD) coronary artery. The needle was then cut from the suture, and the two ends of the 8–0 suture were then threaded through a 0.5-mm piece of PE-10 tubing (Becton Dickinson, Sparks, MD), forming a loose snare around the LAD. The PE-10 tubing was previously soaked for 24 hours in 100% ethanol. Each end of the suture was

then threaded through the end of a size 3 Kalt suture needle (Fine Science Tools, Foster City, CA), and exteriorized through each side of the chest wall. The chest was closed with 3 interrupted stitches using 6–0 Prolene, carefully avoiding pneumothorax, and the animal was removed from the respirator. The ends of the exteriorized 8–0 suture were tucked under the skin, which was then also closed with 6–0 Prolene. The endotracheal tube was withdrawn, and the animal was kept warm with a heat lamp and allowed to breathe 100% oxygen via nasal cone until full recovery of consciousness.

Seven to ten days postinstrumentation, the animals were anesthetized with 1.5% MAC isoflurane in 1 l/min oxygen flow under spontaneous breathing. The extremities were taped to a lead II electrocardiogram (ECG) board to measure S-T elevations during the I/R protocol. The skin above the chest wall was then re-opened. The 8–0 suture, which had been previously exteriorized outside the chest wall and placed under the skin, was cleared of all debris from the skin and chest, and carefully taped to heavy metal picks. Occlusion of the LAD was accomplished by gently pulling the heavy metal picks apart until an S-T elevation appeared on the ECG.



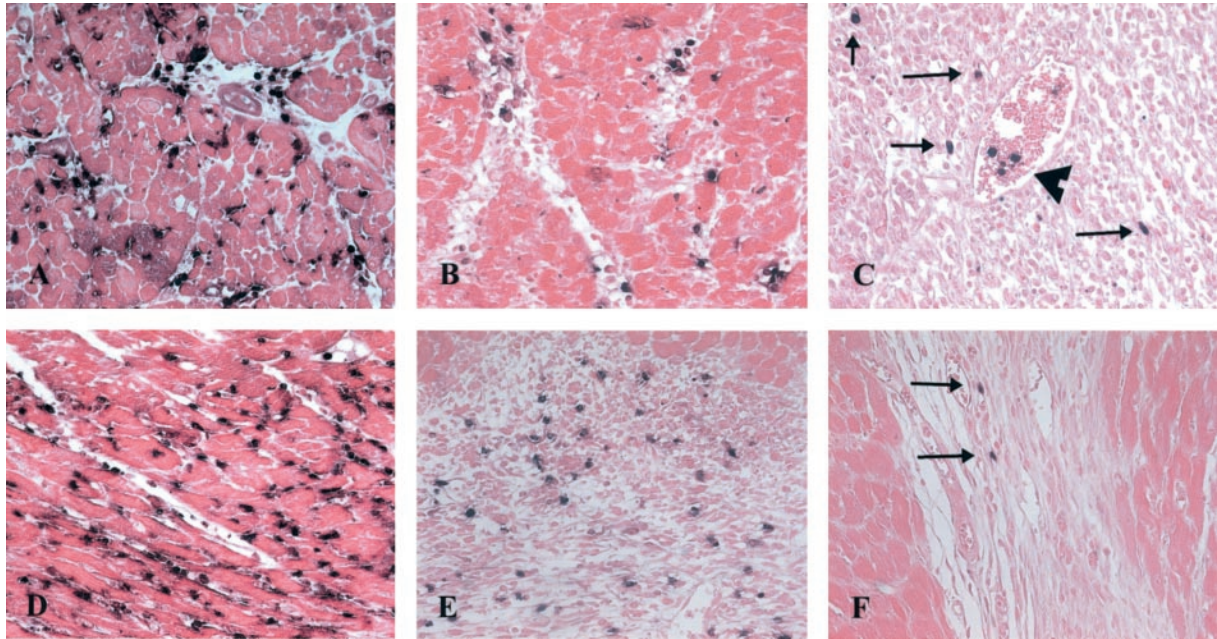


**Figure 2.** Neutrophil immunohistochemistry in reperfused canine (A–C) and mouse (D–F) infarcts. Dog neutrophils were identified using the monoclonal anti-canine neutrophil antibody SG8H6 and mouse neutrophils were labeled with a rat anti-mouse neutrophil antibody. Canine neutrophils rapidly infiltrate the infarct after 24 hours of reperfusion (A), but their number decreases significantly after 72 hours of reperfusion (B). Few neutrophils are found in dog infarcts after 7 days of reperfusion (C, arrows). A large pericyte-poor vessel is noted (arrowhead), containing three intravascular neutrophils. A similar time course is noted in mouse infarcts: abundant neutrophils are found in the infarct after 24 hours of reperfusion (D), but decrease significantly after 72 hours (E). Neutrophils are rare in mouse infarcts after 7 days of reperfusion (F, arrows). Counterstained with eosin (magnification,  $\times 400$ ).

The ECG was constantly monitored throughout the entire ischemic interval to ensure persistent ischemia. After 1 hour of coronary occlusion, reperfusion was accomplished by pushing the metal picks toward the animal,

cutting the suture close to the chest wall, and removing it completely. Subsequently, the skin was closed with a 6–0 Prolene and the animals were kept in the vivarium until the end of the reperfusion interval. At the end of the experiment, mice were anesthetized with sodium pentobarbital overdose the chest was opened and the heart was immediately excised, fixed in Z-fix (Anatech Ltd., Battle Creek, MI) and embedded in paraffin for histological studies, or snap frozen and stored at  $-80^{\circ}\text{C}$  for RNA isolation. Sham animals were prepared identically without undergoing myocardial infarction protocols. Animals used for histology underwent 6-hour, 24-hour, 72-hour, 7-day, and 14-day reperfusion protocols (8 animals per group). To identify mast cells in the murine heart, additional animals underwent 3, 5, 7 and 14 days of reperfusion (5 animals per group) and were fixed in Carnoy's to ensure detection of the formalin sensitive mast cell population. Mice used for RNA extraction underwent 3 hours, 6 hours, 24 hours, 72 hours, and 7 days of reperfusion (8 animals per group).

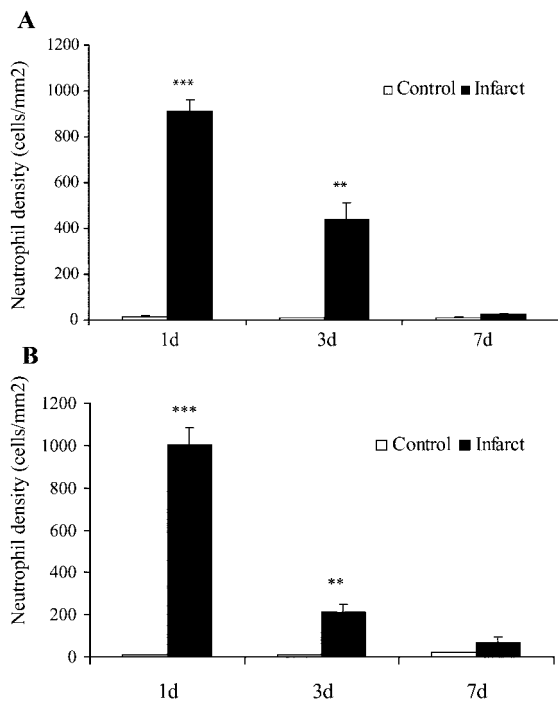


**Figure 3.** Quantitative analysis of neutrophil density in reperfused murine (A) and canine infarcts (B). Neutrophil infiltration in both mouse and dog infarcts is robust but transient, decreasing after 3 days of reperfusion. Neutrophil density in infarcts after 7 days of reperfusion is very low. \*\*\*,  $P < 0.001$ , \*\*,  $P < 0.01$ .

#### Canine Model

An established protocol of canine circumflex coronary occlusion/reperfusion was used.<sup>11,12</sup> Healthy dogs were instrumented with a hydraulic occluder and underwent 1 hour of coronary occlusion, followed by 24 hours, 72 hours, 5 days, and 7 days of reperfusion (5 animals per group). After the reperfusion periods, hearts were stopped by the rapid intravenous infusion of 30 mEq of KCl and removed from the chest for sectioning from apex to base into four transverse rings  $\sim 1$  cm in thickness.

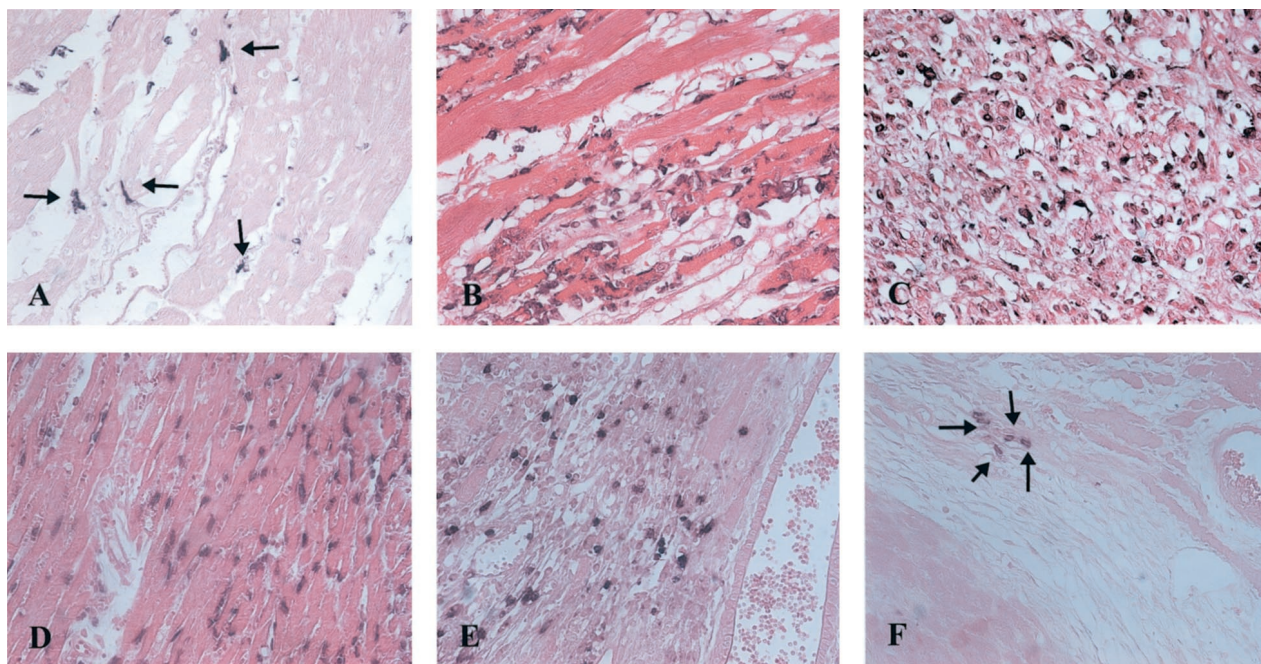


**Figure 4.** Macrophage identification in reperfused canine (A–C) and mouse infarcts (D–F) using the monoclonal antibodies PM-2K (for the dog), and F4/80 (for the mouse). Canine macrophages progressively accumulate in the infarct after 24 hours (A, arrows) to 72 hours (B) of reperfusion, peaking after 7 days of reperfusion (C). In contrast, murine macrophages peak after 24 hours of reperfusion (D), remain abundant after 72 hours (E) and decrease significantly after 7 days of reperfusion (F, arrows). Sections counterstained with eosin (magnification,  $\times 400$ ).

Tissue samples were isolated from infarcted or normally perfused myocardium based on visual inspection. Myocardial segments were fixed in B\*5<sup>13</sup> or Carnoy's fixative for histological analysis.

### *Immunohistochemistry and Histology*

Samples from mouse myocardium were fixed in zinc-formalin (Z-fix; Anatech, Battle Creek, MI), and embedded in paraffin. Sections were cut at 3  $\mu\text{m}$  and stained immunohistochemically with the following antibodies: monoclonal anti- $\alpha$  smooth muscle actin ( $\alpha$ -SMA) antibody (Sigma, St. Louis, MO), rat anti-mouse neutrophil antibody (Serotec, Oxford, UK), rat anti-mouse macrophage antibody F4/80 (Research Diagnostics Inc, Flanders, NJ),<sup>14</sup> and rat anti-mouse CD31 antibody (PharMingen, San Diego, CA).<sup>15</sup> Staining was performed using a peroxidase-based technique with the Vectastain ELITE rat kit (Vector Laboratories, Burlingame, CA) and developed with diaminobenzidine (DAB)+nickel (Vector Laboratories). The Mouse on Mouse (MOM) kit (Vector Laboratories) was used for  $\alpha$ -SMA immunohistochemistry. For CD31 staining, sections were pretreated with trypsin and staining was performed using the tyramide signal amplification (TSA) kit (Perkin Elmer, Boston, MA) as previously described.<sup>16</sup> Slides were counterstained with eosin and examined in a Zeiss microscope equipped with a Leaf Lumina digital camera. To identify mast cells additional mouse hearts were fixed in Carnoy's and the sections were stained with toluidine blue as previously described.<sup>14,17</sup>

Canine samples were fixed in B\*5 fixative and sections were stained with the following antibodies: monoclonal anti- $\alpha$  smooth muscle actin antibody (Sigma),<sup>18</sup> monoclonal anti-canine neutrophil antibody SG8H6<sup>19</sup> (a gift from Dr. C. W. Smith, Baylor College of Medicine), and mouse anti-human CD31 antibody (Dako, Carpinteria, CA).<sup>20</sup> To identify macrophages, we used immunohistochemical staining with the mouse anti-human macrophage antibody PM-2K (Biogenesis, Kingston, NH), which cross-reacts with canine species<sup>21</sup> and detects infarct macrophages as we have previously demonstrated.<sup>22</sup> Staining of canine tissue was performed using a peroxidase-based technique with the Vectastain ELITE mouse kit (Vector Laboratories) and developed with DAB+nickel (Vector Laboratories). Canine cardiac mast cells were identified using toluidine blue staining as previously described.<sup>17</sup>

Quantitative analysis of mast cell density was performed by counting the number of toluidine blue positive mast cells in control and infarct areas. Macrophage quantitation was performed by counting the number of F4/80 positive cells in mice and PM-2K positive cells in dogs. Neutrophil quantitation was performed by counting the number of neutrophils identified in canine and murine hearts using the specific anti-neutrophil antibodies. Mast cell, neutrophil and macrophage density was expressed as cells/mm<sup>2</sup>. Microvascular density was assessed by counting the number of CD31-positive microvascular profiles in infarcted and noninfarcted myocardium.  $\alpha$ -SMA stained area was quantitated as a percentage of the total area of infarcted or control myocardium using



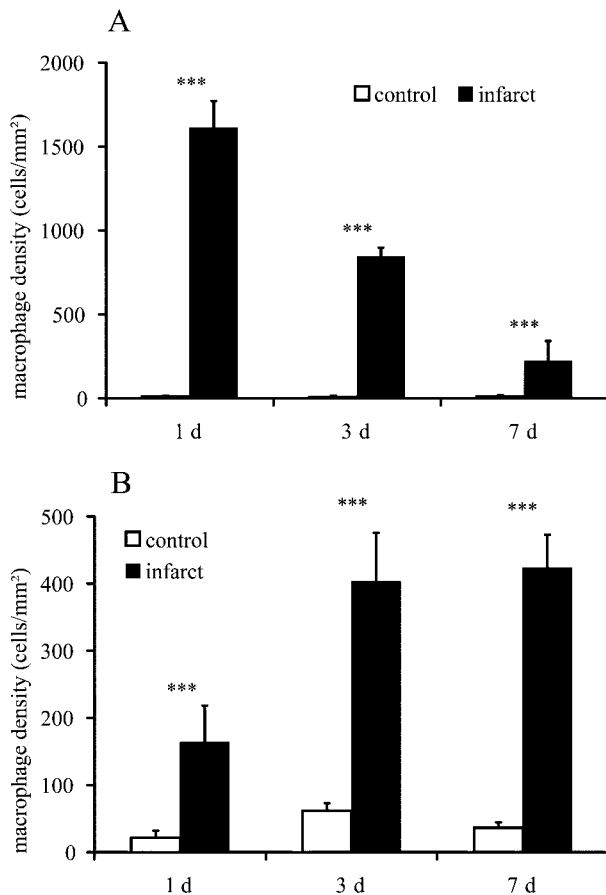


**Figure 5.** Quantitative analysis of macrophage density in reperused murine (A, F4/80 staining) and canine infarcts (B, PM2K staining). Macrophage accumulation in reperused mouse infarcts is robust but transient, decreasing after 7 days of reperfusion. In contrast, macrophage infiltration in dog infarcts is sustained, peaking after 7 days reperfusion. \*\*\*,  $P < 0.001$ .

Image Pro software (Media Cybernetics Inc., Silver Spring, MD).

### RNA Extraction

All solutions for RNA analysis were treated with 0.1% diethylpyrocarbonate and sterilized or prepared in diethylpyrocarbonate-treated water. Glassware was baked at 240°C for 5 hours to remove trace RNases. Total RNA was isolated from whole mouse heart according to the acid-guanidium-thiocyanate-phenol-chloroform. Briefly, whole hearts were homogenized in RNA STAT-60 solution (Tel-Test, Friendswood, TX). For RNA extraction, 0.2 volumes of R-chloroform were then added per volume of homogenate. This mixture was incubated on ice for 15 minutes and then spun at  $12,000 \times g$  for 15 minutes at 4°C. The supernatant was transferred to another tube, and an equal volume of isopropanol was added for RNA precipitation overnight at 4°C. The tubes were then spun at  $12,000 \times g$  for 15 minutes at 4°C, and the supernatant was decanted. The pellet was washed twice with 75% ethanol, briefly dried, and dissolved in 0.1% diethylpyrocarbonate-treated water. Quantification and purity of RNA was assessed by  $A_{260}/A_{280}$  UV absorption, and

RNA samples with ratios above 1.9 were used for further analysis.

### Ribonuclease Protection Assay

The mRNA expression level of the chemokines monocyte chemoattractant protein (MCP)-1, macrophage inflammatory protein (MIP)-1 $\alpha$ , MIP-1 $\beta$ , MIP-2, and interferon- $\gamma$  inducible protein (IP)-10, the IP-10 receptor, CXCR3, the cytokines tumor necrosis factor (TNF)- $\alpha$ , interleukin (IL)-1 $\beta$ , IL-6, leukemia inhibitory factor (LIF) and IL-10, the growth factors transforming growth factor (TGF)- $\beta$ 1, 2, and 3, stem cell factor (SCF), granulocyte macrophage-colony stimulating factor (GM-CSF) and macrophage-colony stimulating factor (M-CSF), the adhesion molecules intercellular adhesion molecule (ICAM)-1, CD31/platelet endothelial cell adhesion molecule (PECAM)-1 and E-selectin, the matricellular protein osteopontin (OPN)-1, and the cytokine receptors IL-10 receptor (IL-10R), and GM-CSF receptor was determined using a ribonuclease protection assay (RiboQuant; PharMingen) according to the manufacturer's protocol. Phosphorimaging of the gels was performed (Storm 860; Molecular Dynamics, Sunnyvale, CA) and signals were quantified using Image QuANT software and normalized to the ribosomal protein L32 mRNA.

### Statistical Analysis

All data are presented as means  $\pm$  SEM. Comparison between the groups was done using analysis of variance with a Student's–Newman-Keuls corrected post hoc analysis. Differences with  $P < 0.05$  were considered significant.

## Results

### Myocyte Replacement Occurs Faster in Murine Infarcts than in Canine Infarcts

Reperused myocardial infarction in both mice and dogs is associated with rapid infiltration of the injured myocardium with inflammatory cells, accompanied by clearance of necrotic cardiomyocytes. Extensive leukocyte extravasation is noted in both murine and canine infarcts after 24 hours of reperfusion (Figure 1, A and E). After 72 hours of reperfusion, murine infarcts demonstrate almost complete replacement of injured cardiomyocytes with inflammatory cells (Figure 1F). In contrast, canine infarcts demonstrate a significantly slower progression of myocyte replacement and persistent presence of significant numbers of contracted cardiomyocytes surrounded by an inflammatory infiltrate (Figure 1B). After 7 days of reperfusion, murine infarcts show thinning and decreased cellular content (Figure 1G), whereas canine infarcts are filled with inflammatory cells (Figure 1C). Further loss of cellular content is noted in mouse infarcts after 14 days of reperfusion (Figure 1H), whereas the dog infarct (Figure 1D) is still highly cellular.

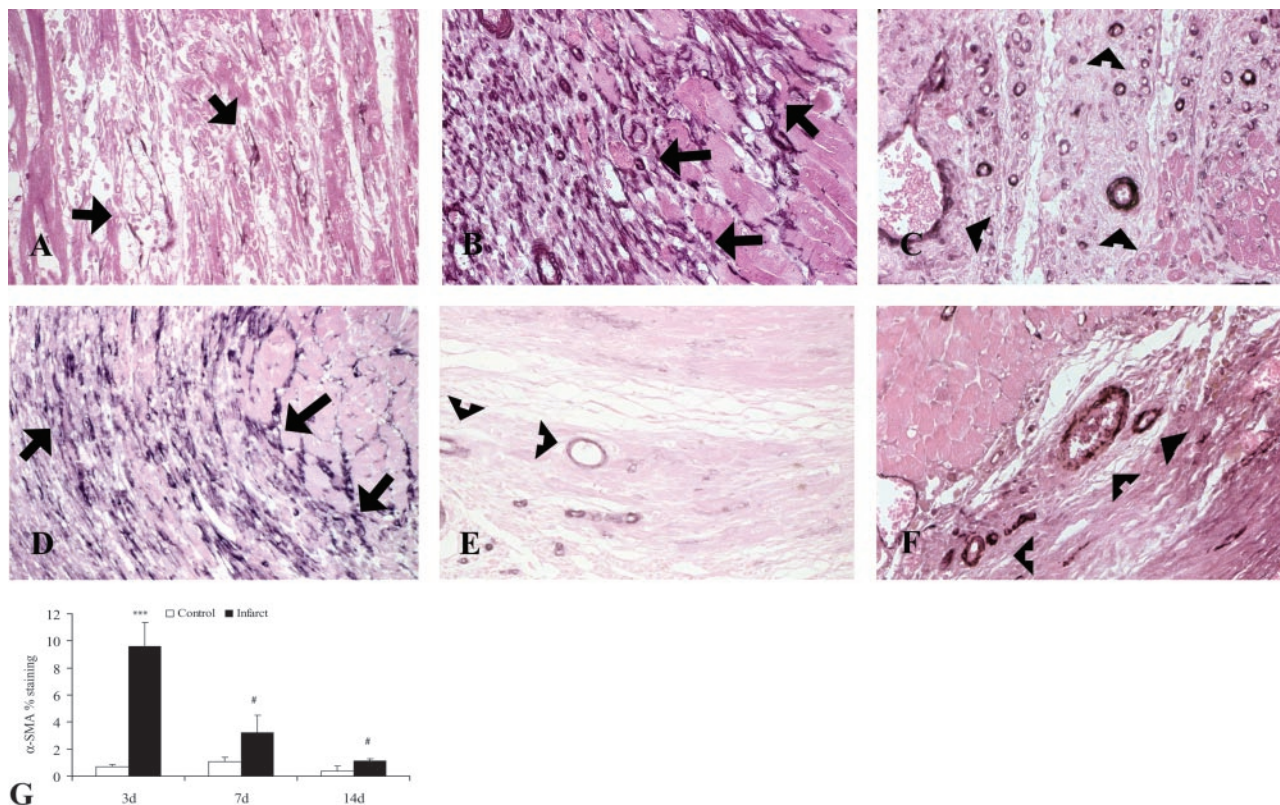


**Figure 6.**  $\alpha$ -smooth muscle actin ( $\alpha$ -SMA) staining in reperfused canine (A–C) and murine infarcts (D–F). Dog infarcts show occasional  $\alpha$ -SMA positive spindle-shaped cells (arrows) after 72 hours of reperfusion (A). These cells are phenotypically modulated fibroblasts, termed myofibroblasts. Myofibroblast accumulation increases dramatically after 7 days of reperfusion in the canine infarct (B, arrows). After 14 days of reperfusion  $\alpha$ -SMA staining is predominantly localized in smooth muscle cells and pericytes coating maturing wound neovessels (C, arrowheads). In contrast, mouse infarcts exhibit a rapid and transient myofibroblast response. After 72 hours of reperfusion mouse infarcts show extensive myofibroblast infiltration (D, arrows). However, after 7 days of reperfusion myofibroblasts in the infarcted mouse heart significantly decrease and  $\alpha$ -SMA staining is predominantly localized in pericyte-coated vessels (E, arrowheads) indicating rapid maturation of the infarct neovasculature.  $\alpha$ -SMA immunoreactivity remains localized in vascular structures (arrowheads) after 14 days of reperfusion (F, arrowheads). **G:** Quantitative analysis of  $\alpha$ -SMA staining in healing mouse infarcts. Infarct  $\alpha$ -SMA % staining peaks after 3 days of reperfusion (\*\*\*,  $P < 0.001$  compared with non-infarcted heart) and decreases significantly after 7–14 days of reperfusion (#,  $P < 0.01$  compared with % staining after 3 days of reperfusion).

### Time Course of Neutrophil, Macrophage, and Myofibroblast Accumulation in Canine and Murine Infarcts

Reperfused canine and murine infarcts demonstrate rapid infiltration with inflammatory leukocytes, leading to the formation of granulation tissue with a high cellular content. Neutrophils rapidly infiltrate both murine and canine infarcts (Figures 2 and 3) peaking after 24 hours of reperfusion, but are rarely found after 7 days of reperfusion (Figure 2, C and F). Reperfused mouse infarcts exhibit a transient increase in macrophage and fibroblast accumulation, followed by decreased cellular content after 7 to 14 days of reperfusion. Macrophage density rapidly increases after 6 hours of reperfusion (data not shown), peaking after 24 hours of reperfusion (macrophage density  $1805 \pm 185.5$  cells/mm<sup>2</sup>; Figures 4D and 5A). Subsequently as the scar matures, a significant decrease in macrophage density is noted after 7 days (density  $136.9 \pm 56.9$  cells/mm<sup>2</sup>,  $P < 0.01$  vs. 24 hours; Figures 4F and 5A). Myofibroblasts, identified as spindle-shaped  $\alpha$ -smooth muscle actin positive cells, accumulate in the border zone of the mouse infarct after 72 hours of reperfusion (Figure 6D). Myofibroblast infiltration in in-

farcted mice appears to be a transient response: after 7 and 14 days of reperfusion the mature mouse infarct has relatively low myofibroblast content and decreased  $\alpha$ -SMA % staining when compared with 3-day infarcts (Figure 6, E–G).

In contrast, canine infarcts show a progressive increase in macrophage and myofibroblast accumulation, peaking after 7 days of reperfusion. Macrophage density in reperfused canine infarcts is significantly higher than in control myocardial areas after 24 hours of reperfusion and continues to increase for the following 6 days, (Figure 4, A–C, and Figure 5B). In addition, dog infarcts demonstrate a delayed and sustained myofibroblast response, which is first noted after 72 hours of reperfusion and peaks after 7 days (Figure 6, A and B). As we have previously demonstrated  $\alpha$ -SMA % staining in the canine infarct peaks after 5 to 14 days of reperfusion, decreasing significantly after 3 to 4 weeks of reperfusion<sup>18</sup> (Table 1).

### Mast Cells Infiltrate Canine but Not Murine Myocardial Infarcts

Using histochemical staining with toluidine blue, we examined the presence of mast cells in canine and murine

**Table 1.** Pathologic Features of Reperfused Myocardial Infarcts: Comparison of a Canine and a Murine Model

Feature	Mouse	Dog
Granulation tissue formation	Rapid formation of granulation tissue; injured cardiomyocytes replaced with granulation tissue after 72 h of reperfusion in animals undergoing 1-h coronary occlusion protocols (Figure 1)	Slower formation of granulation tissue; injured cardiomyocytes are replaced with granulation tissue after 120 h of reperfusion in animals undergoing 1-h coronary occlusion protocols
Neutrophil recruitment	Rapid and transient neutrophil infiltration (Figures 2, 3)	Rapid and transient neutrophil infiltration (Figures 2, 3)
Macrophage recruitment	Rapid influx of monocytes; macrophage accumulation peaks early and decreases significantly after 7 days of reperfusion (Figures 4, 5)	Rapid influx of monocytes; sustained macrophage accumulation peaks after 7 days of reperfusion (Figures 4, 5)
Myofibroblast accumulation	Maximal myofibroblast accumulation after 72 h of reperfusion; myofibroblast density decreases after 7 days of reperfusion (Figure 6)	Low number of myofibroblasts after 72 h of reperfusion (Figure 6); myofibroblast accumulation peaks after 7 days of reperfusion <sup>18</sup>
Mast cell recruitment	No increase in mast cell density found in healing mouse infarcts (Figure 7)	Significant mast cell accumulation in infarcted dog hearts after 72 h of reperfusion <sup>23</sup> ; mast cell infiltration persists for at least 2 weeks after coronary occlusion
Wound angiogenesis	Low capillary density in the infarcted area after 7–14 days of reperfusion (<500 microvessels/mm <sup>2</sup> ); formation of large dilated vessels; progressive coating of the neovessels with pericytes; coating and maturation of infarct neovessels complete after 14 days of reperfusion (Figure 8)	High capillary density in the infarcted area after 7–14 days of reperfusion (>1500 microvessels/mm <sup>2</sup> ) <sup>18</sup> ; formation of large dilated vessels; progressive coating of the neovessels with pericytes <sup>20</sup> ; coating and maturation of infarct neovessels continues one month after coronary occlusion <sup>20</sup>
Pro-inflammatory cytokine expression	Transient induction of IL-1 $\beta$ , IL-6, and TNF- $\alpha$ (Figure 9)	Transient induction/release of IL-6 <sup>31</sup> and TNF- $\alpha$ <sup>11</sup>
Inhibitory cytokine expression	Early induction of IL-10 persists for at least 72 h of reperfusion; up-regulation of TGF- $\beta$ 1, $\beta$ 2, $\beta$ 3 (Figure 9)	Late induction of IL-10, peaks after 96 h of reperfusion <sup>12</sup>
Growth factor expression	High-level expression of M-CSF mRNA in the non-infarcted heart; modest M-CSF up-regulation in infarcts; no SCF induction; the infarct microenvironment may not support sustained macrophage and mast cell survival (Figure 10)	Marked M-CSF <sup>22</sup> and SCF <sup>23</sup> mRNA up-regulation in canine infarcts; these factors may support mast cell and macrophage survival
Adhesion molecule expression	Rapid and transient induction of ICAM-1 and E-selectin (Figure 10)	Rapid induction of ICAM-1 <sup>28</sup>
Chemokine expression	Rapid and transient expression of MCP-1, MIP-1 $\alpha$ , MIP-1 $\beta$ , IP-10 (Figure 11)	Rapid expression of MCP-1 <sup>34</sup> , IL-8 <sup>33</sup> , IP-10 <sup>35</sup> ; MCP-1 up-regulation persists for at least 48 h <sup>34</sup>

myocardial infarcts. Noninfarcted canine myocardium contains a resident mast cell population, while infarcted areas are infiltrated after 3 (Figure 7A) and 7 days (Figure 7A), with significant number of mast cells (Figure 7C), as described in detail in a previous study.<sup>17,23</sup> Mast cell numbers in the infarcted areas remain elevated after 14 days of reperfusion (Figure 7C). In contrast, normal mouse myocardium has few mast cells, predominantly located in the epicardial third of the left ventricular wall. Mast cell infiltration was not found in the mouse infarct after 3 (Figure 7D) and 7 days of reperfusion (Figure 7E), and the mast cell density remained low and comparable to the density in control areas (Figure 7F).

### *The Infarct Vasculature in Mouse and Canine Infarcts*

Infarct healing in both mice and dogs is associated with an angiogenic response leading to formation of

neovessels in the infarcted territory. Dilated pericyte-poor “mother vessels” are present in both murine and canine infarcts; they are, however, more abundant in mice (Figure 8). In both mice and dogs, infarct neovessels undergo a maturation process leading to the formation of pericyte coated vessels and regression of many capillaries. Mouse infarcts exhibit a low microvascular density after 7 days of reperfusion (infarct:  $492.3 \pm 45.1$  microvessels/mm<sup>2</sup> vs. non-infarcted area:  $2659 \pm 236.9$  microvessels/mm<sup>2</sup>) showing a significant number of mature pericyte-coated vessels (Figure 6E). In contrast, at the same time point, canine infarcts have a high capillary density (more than 1500 microvessels/mm<sup>2</sup>)<sup>18</sup> and relatively few vessels with a muscular coat (Figure 8B). Vascular maturation and acquisition of a muscular coat in canine infarct neovessels occurs after 4 to 8 weeks of reperfusion and is accompanied by a decrease in capillary density.<sup>20</sup>



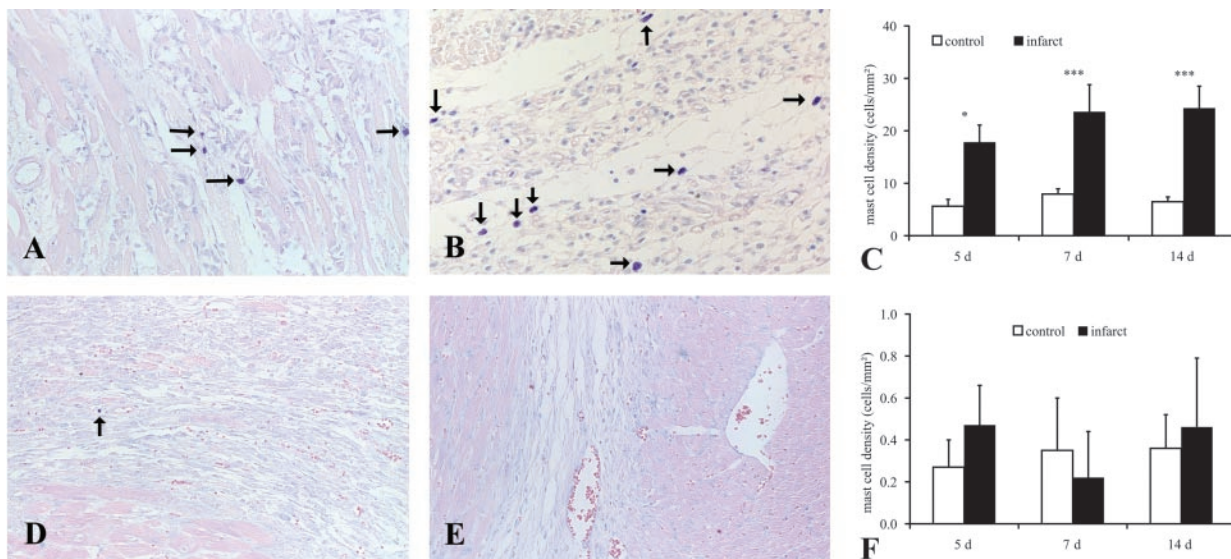


**Figure 7.** Mast cells were identified in canine (**A, B**) and murine infarcts (**D, E**) using toluidine blue staining. Canine infarcts show significant mast cell accumulation after 3 days of reperfusion (**A, arrows**). Mast cell accumulation increases further after 7 days of reperfusion (**B, arrows**). In contrast, mouse infarcts have few mast cells in infarcted areas (**arrow**) after 3 (**D**), and 7 days of reperfusion (**E**). Diagrams show quantitative analysis of mast cell density in canine (**C**) and murine (**F**) infarcts. \*,  $P < 0.05$ ; \*\*\*,  $P < 0.001$ .

### Induction of Cytokines, Chemokines, and Adhesion Molecules in Mouse Infarcts

To identify molecular signals responsible for the cellular changes noted in murine infarcts we examined the levels of mRNA expression for various inflammatory mediators in infarcted mouse hearts and compared them with sham-operated controls. Infarcted mice demonstrated a robust inflammatory response associated with significantly increased synthesis of cytokines, chemokines, and adhesion molecules. IL-1 $\beta$  and IL-6 mRNA expression was markedly increased in mouse infarcts after 6 hours of reperfusion (>20-fold compared with sham-operated controls; Figure 9, A–C). Expression of TNF- $\alpha$  and LIF was also significantly increased, but to a lesser degree (threefold increase vs. sham animals; Figure 9, A and C). Cytokine expression in the infarcted mouse hearts rapidly returned to sham levels after 24 to 72 hours of reperfusion. IL-10, an inhibitory cytokine with an important role in pro-inflammatory cytokine regulation was also markedly induced in mouse infarcts peaking after 6 hours of reperfusion (sixfold increase vs. sham; Figure 9E). However, in contrast with the transiently increased expression of TNF- $\alpha$ , IL-6 and IL-1 $\beta$ , IL-10 mRNA levels remained elevated for at least 3 days after reperfusion. mRNA expression of the TGF- $\beta$  isoforms was also increased in infarcted mouse hearts (Figure 9F). TGF- $\beta$ 1 and - $\beta$ 2 had a similar time course, with significantly elevated mRNA expression after 6 to 72 hours of reperfusion and return to sham levels after 7 days of reperfusion. In contrast, TGF- $\beta$ 3 mRNA synthesis exhibited a delayed response peaking after 3 to 7 days of reperfusion. Induction of pro-inflammatory cytokines was associated with increased mRNA synthesis of the adhesion molecules ICAM-1 (Figure 10B) and E-selectin (sixfold vs. sham; Figure 10C) that peaked after 6 hours of reperfusion and returned to sham levels after 24 hours of reperfusion. In

contrast, PECAM-1 mRNA expression was high in sham mouse hearts and did not change significantly in reperused infarcts (Figure 10A). In addition, a robust transient up-regulation of the chemokines MIP-1 $\alpha$ , MIP-1 $\beta$ , MIP-2, MCP-1 (Figure 11) and IP-10 was noted in the mouse infarct. MIP-2, MCP-1 and MIP-1 $\beta$  mRNA synthesis was markedly induced in mouse infarcts (>30-fold vs. sham animals), peaking after 6 hours of reperfusion. mRNA expression of all chemokines rapidly decreased after 24 to 72 hours of reperfusion, except for IP-10, which exhibited a second smaller peak after 72 hours of reperfusion. Expression of the IP-10 receptor, CXCR3, also increased after 3 to 6 hours of reperfusion (Figure 11A). We have previously described up-regulation of cytokines, chemokines and adhesion molecules in experimental myocardial infarction in dogs as well and, while similar, their time courses are distinct (Table 1). It should be noted, however, that canine infarcts also exhibit sustained up-regulation of the growth factors M-CSF<sup>22,24</sup> and SCF,<sup>23</sup> which may have an important role in supporting survival and maturation of macrophages and mast cells. In contrast, infarcted mouse hearts demonstrate only a small transient increase (1.5-fold after 3 hours of reperfusion) of M-CSF mRNA levels compared with sham-operated animals (Figure 10D) and show no SCF induction (Figure 10E). Although a modest up-regulation of GM-CSF is noted after 3–6 hours of reperfusion (Figure 10A), GM-CSF mRNA levels are very low in both sham and infarcted murine hearts (<2% of the mRNA levels of the housekeeping gene L32). In addition the matricellular protein OPN-1, a remodeling-associated gene induced in healing canine infarcts,<sup>24</sup> was markedly up-regulated in mouse infarcts peaking after 24 to 72 hours of reperfusion (Figure 9A). Finally, expression of the GM-CSF and IL-10 receptors did not change significantly in infarcted mouse hearts.



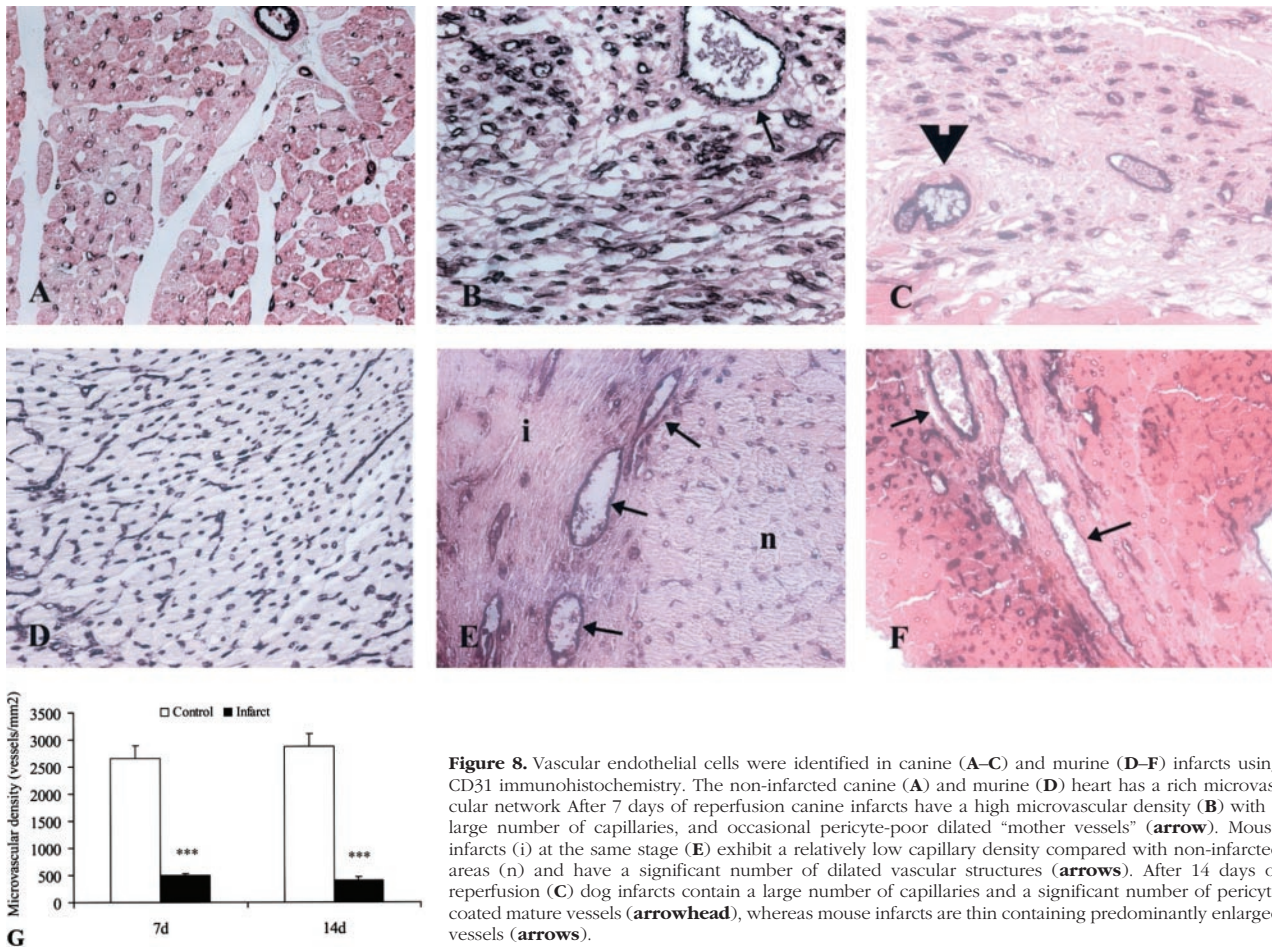


**Figure 8.** Vascular endothelial cells were identified in canine (A–C) and murine (D–F) infarcts using CD31 immunohistochemistry. The non-infarcted canine (A) and murine (D) heart has a rich microvascular network. After 7 days of reperfusion canine infarcts have a high microvascular density (B) with a large number of capillaries, and occasional pericyte-poor dilated “mother vessels” (arrow). Mouse infarcts (i) at the same stage (E) exhibit a relatively low capillary density compared with non-infarcted areas (n) and have a significant number of dilated vascular structures (arrows). After 14 days of reperfusion (C) dog infarcts contain a large number of capillaries and a significant number of pericyte coated mature vessels (arrowhead), whereas mouse infarcts are thin containing predominantly enlarged vessels (arrows).

## Discussion

Investigations using large animal models of experimental myocardial infarction have allowed a detailed descriptive analysis of the pathological process of infarction and have significantly contributed to our understanding of the pathobiology of ischemic myocardial injury. Recently, the technological advances in gene targeting and transgenic approaches led to the development of murine models of experimental myocardial infarction that could prove valuable in dissecting the role of specific genes in infarction and cardiac repair.<sup>25</sup> However, extrapolation of the conclusions derived from murine studies to the human pathological process implies similar mechanisms in both species. Although mice and men share a large number of highly conserved genes that regulate fundamental aspects of cardiovascular morphogenesis and pathophysiology, their inherent differences suggest that species variability may ultimately become a critical consideration in interpreting conclusions derived from murine studies.<sup>3</sup> For example, the electrophysiology of the mouse heart as well as the thrombosis and coagulation cascades are quite distinct from that of the human making the mouse an unsuitable model for questions in these fields.<sup>3</sup> The current study examines the pathological features of reperfused myocardial infarcts in mice and compares the molecular and cellular events involved in murine and

canine infarct healing. Both closed chest infarct models (murine and canine) were developed in our laboratory to minimize the influence resulting from acute operating trauma. Our current study demonstrates that mouse infarcts, much like canine infarcts, exhibit a robust inflammatory response, with increased expression of cytokines, adhesion molecules, and chemokines. However, murine infarcts show a more rapid progression of the inflammatory process with formation of granulation tissue and myocyte replacement after 72 hours of reperfusion. Unlike canine infarcts, reperfused infarcted mouse hearts show only transient macrophage infiltration and no significant mast cell accumulation, leading to wounds with a relatively low cellular content after 7 days of reperfusion. The relative absence of chronic inflammatory cells in the mature mouse infarct may be related to the lack of significant induction of growth factors, such as M-CSF and SCF, necessary to support survival and maturation of macrophages and mast cells.

### *Induction of Inflammatory Mediators in Reperfused Mouse Infarcts*

In large mammals experimental myocardial infarction is associated with an inflammatory response which ultimately leads to healing and formation of a mature scar

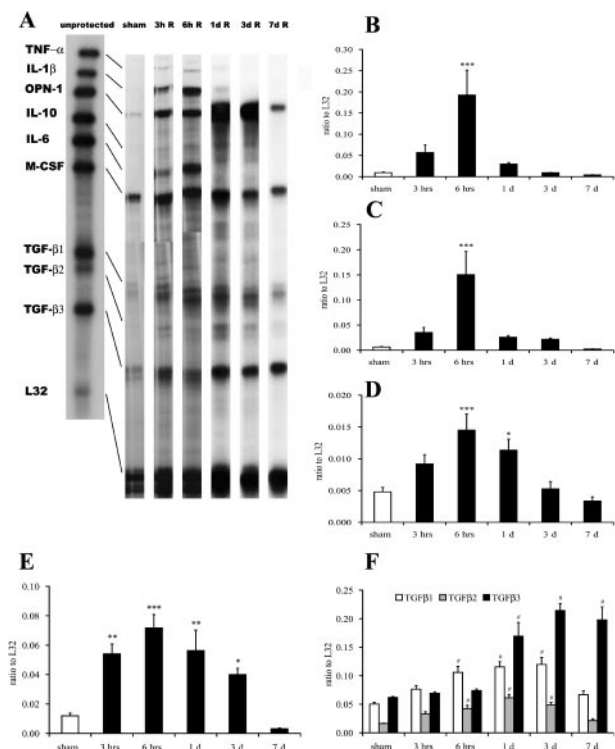


**Figure 9.** Cytokine expression in reperfused murine infarcts. **A:** Representative experiments demonstrate significant up-regulation of the pro-inflammatory cytokines IL-1 $\beta$ , IL-6, and TNF- $\alpha$  after 3 to 6 hours of reperfusion. The inhibitory cytokines IL-10 and TGF- $\beta$ , and the matricellular protein osteopontin (OPN)-1, a marker of interstitial remodeling, are also upregulated in mouse infarcts. mRNA expression of IL-1 $\beta$  (**B**), IL-6 (**C**), and TNF- $\alpha$  (**D**) peaks after 6 hours of reperfusion but decreases significantly after 3 days of reperfusion. \*,  $P < 0.05$ ; \*\*\*,  $P < 0.001$ . mRNA E, F: Quantitative analysis of IL-10 (**E**) and TGF- $\beta$ 1, 2, and 3 (**F**) mRNA expression in reperfused murine infarcts. IL-10, TGF- $\beta$ 1, and TGF- $\beta$ 2 are transiently induced during reperfusion, in contrast to the later and more persistent up-regulation of TGF- $\beta$ 3. \*,  $P < 0.05$ ; \*\*,  $P < 0.01$ ; \*\*\*,  $P < 0.001$ , #,  $P < 0.01$ .

(Table 1).<sup>26,27</sup> Adhesion molecules such as ICAM-1 are rapidly induced in canine infarcts<sup>28,29</sup> and may have an important role in leukocyte recruitment and neutrophil-mediated injury.<sup>30</sup> Adhesion molecule expression may be mediated through up-regulation and release of cytokines such as TNF- $\alpha$ <sup>11</sup> and IL-6.<sup>31</sup> In addition, expression of the chemokines IL-8, MCP-1 and IP-10 has been a prominent feature of rabbit and canine infarcts<sup>32-35</sup> and may regulate recruitment of inflammatory leukocytes in the ischemic myocardium. Much like infarcts in larger mammal species, mouse infarcts exhibit a robust and transient expression of inflammatory mediators. Expression of neutrophil and mononuclear cell chemotactic factors such as the chemokines MIP-2, MCP-1, MIP-1 $\alpha$ , MIP-1 $\beta$ , and IP-10 is highly induced in mouse infarcts and may critically regulate inflammatory cell recruitment. In addition, the pro-inflammatory cytokines IL-1 $\beta$  and IL-6 are markedly induced in the murine infarct and may contribute to recruitment of inflammatory cells by up-regulating expression of adhesion molecules. Cytokine, chemokine and adhesion molecule expression in mouse infarcts is transient, decreasing significantly after 24 hours of reperfusion. In contrast, canine infarcts exhibit a more sustained expression of certain inflammatory mediators such as ICAM-1, IL-6 and MCP-1. The transient nature of pro-

inflammatory cytokine expression in mouse infarcts may be due to the rapid up-regulation of IL-10 (Figure 9E; Ref. 36) and TGF- $\beta$  (Figure 8B), both potent inhibitory cytokines capable of suppressing TNF- $\alpha$  and IL-1 $\beta$  synthesis. Dogs demonstrate a more delayed and sustained IL-10 response,<sup>12</sup> this may account for the relatively prolonged expression of inflammatory mediators such as ICAM-1<sup>28</sup> and MCP-1<sup>34</sup> reported in various studies. TGF- $\beta$  isoforms in mouse infarcts exhibited differential expression: TGF- $\beta$ 1 and  $\beta$ 2 were induced after 3 hours and their expression significantly decreased after 3 to 7 days of reperfusion, whereas TGF- $\beta$ 3 showed a delayed and sustained induction after 3 to 7 days. TGF- $\beta$  expression in mouse infarcts may be important in regulating matrix deposition, fibroblast differentiation and scar formation. Studies investigating the repair of rat cutaneous wounds demonstrated that TGF- $\beta$ 1 and TGF- $\beta$ 2<sup>37</sup> promote excessive deposition of extracellular matrix proteins that lead to scarring. In contrast, exogenous application of TGF- $\beta$ 3 to these wounds reduced extracellular matrix protein deposition and scarring.<sup>38</sup> Differential expression of TGF- $\beta$  isoforms in infarcts may regulate extracellular matrix remodeling and modulate fibroblast phenotype. Increased and sustained TGF- $\beta$ 3 synthesis during maturation of the scar may prevent excessive accumulation of collagen in the injured heart.

### Macrophages and Mast Cells in Canine and Murine Infarcts

Chemokine induction is a prominent characteristic of the postinfarction inflammatory response in both large mammals<sup>26,39</sup> and mice (Figure 11). It is accompanied by infiltration of the injured myocardium with inflammatory leukocytes, which are involved in phagocytosis of dying cardiomyocytes, synthesis of cytokines and growth factors, and regulation of matrix metalloproteinase activity. Neutrophils rapidly infiltrate the infarcted myocardium in both mice and dogs, but are rarely found after 7 days of reperfusion (Figures 2 and 3). Macrophage density also increases rapidly in both murine and canine infarcts (Figures 4 and 5). However, mouse infarcts exhibit a more rapid and transient infiltration with mononuclear cells, leading to almost complete replacement of cardiomyocytes with granulation tissue after 72 hours of reperfusion. In contrast, canine infarcts after 1 hour of coronary occlusion and 72 hours of reperfusion demonstrate persistent presence of injured cardiomyocytes with minimal replacement by granulation tissue and extensive interstitial inflammatory leukocyte infiltration. Furthermore, macrophage infiltration in mouse infarcts appears to be transient, and macrophage density significantly decreases after 7 days of reperfusion, leading to a thinned scar with relatively low cellular content. In contrast, canine infarcts exhibit high proliferative activity<sup>18</sup> and increased macrophage content after 7 days of reperfusion (Figures 3 and 4). In addition, sustained mast cell infiltration is noted in dog, but not in mouse infarcts after experimental infarction, suggesting that the microenvironment in canine infarcts supports proliferation and survival of resident in-



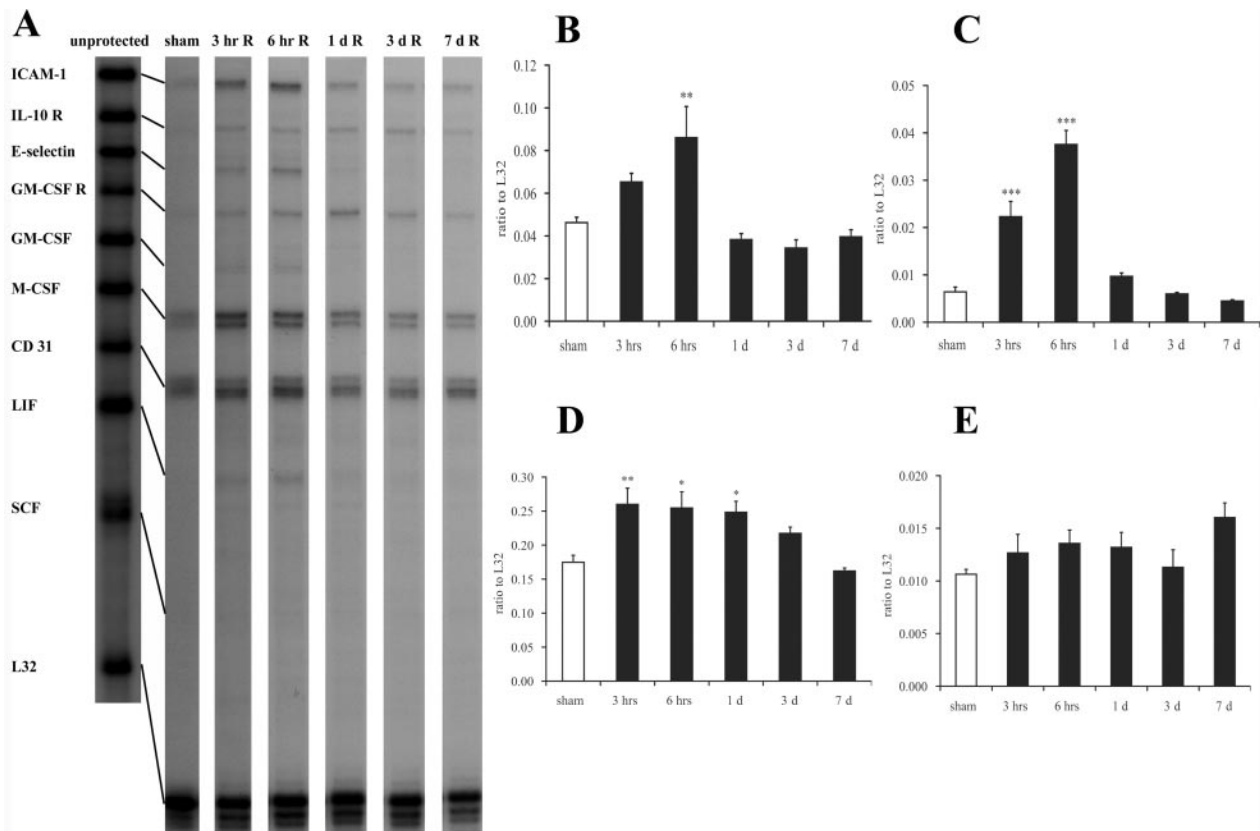


**Figure 10. A:** mRNA expression of the adhesion molecules ICAM-1 and E-selectin and the cytokine LIF is induced in mouse infarcts after 6 hours of reperfusion. In contrast expression of the adhesion molecule CD31/PECAM-1, and the cytokine receptors IL-10R and GM-CSF R do not change significantly after infarction. In addition, infarcted mouse hearts demonstrate a transient increase of M-CSF mRNA levels compared with sham-operated animals and show no SCF induction. **B-E:** Quantitative analysis of ICAM-1 (**B**), E-selectin (**C**), M-CSF (**D**) and SCF (**E**) mRNA levels in mouse infarcts. A modest transient induction of M-CSF (**D**) is found until 24 hours of reperfusion, associated with a transient macrophage accumulation in the infarcted mouse heart. Expression of SCF, a crucial factor for mast cell survival and growth did not show significant increase in murine infarcts (**E**). This finding may explain the absence of mast cell infiltration in healing mouse infarcts (Figure 7). \*\*,  $P < 0.01$ ; \*\*\*,  $P < 0.001$ .

flammatory cells, such as mast cells and macrophages. Mast cell and macrophage accumulation in dog infarcts is associated with significant induction of SCF,<sup>23</sup> a potent chemotactic and survival factor for mast cells, and marked and sustained up-regulation of M-CSF,<sup>22</sup> a growth factor crucial for maturation and proliferation of macrophages. In contrast, murine infarcts exhibit a modest and transient up-regulation of M-CSF and no SCF induction. These findings suggest that although mouse infarcts show high expression of chemotactic factors, they lack expression of growth factors necessary to support a significant population of macrophages and mast cells. The rapid decrease in macrophage numbers may explain the extensive thinning associated with murine infarction.

#### *Myofibroblast Accumulation in Canine and Murine Infarcts*

Tissue repair is associated with accumulation of phenotypically modulated fibroblasts called myofibroblasts.<sup>40</sup> These cells express  $\alpha$ -smooth muscle actin and play an active role in extracellular matrix deposition and metabolism in healing infarcts.<sup>41,42</sup> TGF- $\beta$ 1 expression appears to be important in regulating the phenotypic changes

associated with myofibroblast differentiation.<sup>43</sup> Both canine and murine infarcts exhibit accumulation of myofibroblasts, predominantly located in the infarct border zone. However myofibroblast infiltration in mouse infarcts is rapid and transient, peaking after 72 hours of reperfusion, whereas dogs demonstrate a more delayed and sustained response, with a high number of myofibroblasts after 7 days of reperfusion.<sup>18</sup> Myofibroblast proliferation and growth may require macrophage-derived growth factors, such as TGF- $\beta$ 1 and FGFs. Thus, in canine infarcts the sustained macrophage response may be capable of maintaining an environment favorable for fibroblast growth. In contrast, mouse infarcts quickly reach the maturation phase and demonstrate decreased macrophage density and TGF- $\beta$ 1 expression after 7 days of reperfusion, exhibiting quicker resolution of the granulation tissue.

#### *Mouse Models of Experimental Infarction: Are They Relevant for Human Studies?*

Due to the availability of knockout and transgenic animals, murine models are very attractive tools for investigating the pathogenetic mechanisms involved in cardiovascular disease. Despite the small size of the murine

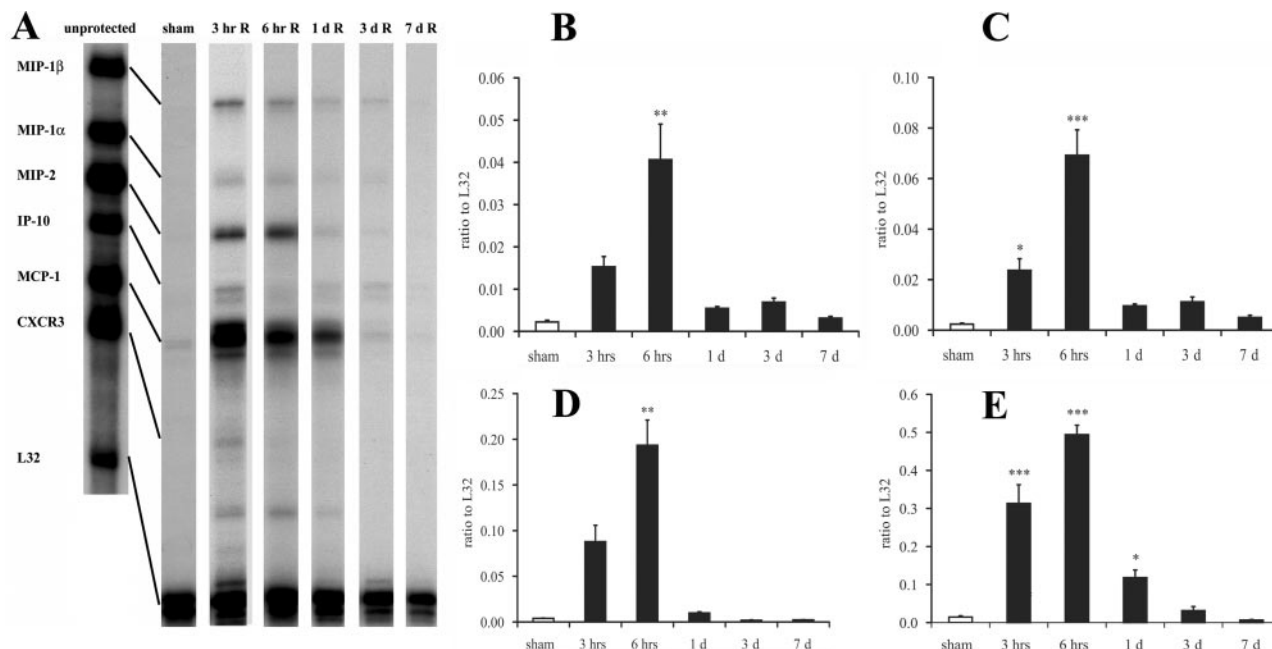


**Figure 11. A:** Chemokine mRNA expression in reperfused mouse infarcts. MIP-1 $\alpha$ , MIP-1 $\beta$ , MIP-2, and MCP-1 follow a similar pattern of transient up-regulation, peaking after 3–6 hours of reperfusion. In addition, IP-10 and its receptor CXCR3 are also induced in mouse infarcts. **B–E:** Quantitative analysis of MIP-1 $\alpha$  (**B**), MIP-1 $\beta$  (**C**), MIP-2 (**D**), and MCP-1 (**E**) expression in canine infarcts. \*,  $P < 0.05$ ; \*\*,  $P < 0.01$ ; \*\*\*,  $P < 0.001$ .

heart, several laboratories have developed reproducible models of myocardial infarction. Given the large potential for species variability, it is important to clearly define whether the mouse displays a conserved response to myocardial injury, when compared with larger mammalian species. Previous studies have reported significant differences in the biology of the inflammatory response between mice and higher mammals. Chemokine profiles, and the response of various cell types to inflammatory cytokines differ significantly between species.<sup>44,45</sup> Recently, Yao and co-workers<sup>46</sup> described species-specific differences in cytokine-induced selectin expression between mice and primates. Furthermore, the heterogeneous morphological and functional characteristics of mast cells between various species have been widely recognized.<sup>14,47</sup> Jugdutt and co-workers<sup>48</sup> have compared the rate of collagen deposition during healing and postinfarction remodeling between dogs and rats and reported that rat infarcts exhibited faster healing and infarct collagen deposition and markedly lower infarct collagen. We found that when considered as a whole, the postinfarction inflammatory response in mice shares many common characteristics with higher mammalian species and is a good model for exploration of cellular and molecular mediators in those events. However, compared with dogs, mice demonstrated a more rapid and transient infiltration with inflammatory leukocytes accompanied by fast replacement of injured cardiomyocytes with granulation tissue. In addition, the microenvironment in healing murine infarcts does not support sustained macrophage and mast cell presence. These important species-specific differences should be considered when extrapolating findings derived from studies using genetically altered mice to the human disease process.

### Acknowledgments

We thank Peggy Jackson, Alida Evans, Sherita Daniel, and Stephanie Butcher for expert technical assistance and Conception Mata and Sharon Malinowski for editorial assistance with the manuscript.

### References

- Jugdutt BI, Hutchins GM, Bulkley BH, Becker LC: Myocardial infarction in the conscious dog: three-dimensional mapping of infarct, collateral flow and region at risk. *Circulation* 1979, 60:1141–1150
- Michael LH, Lewis RM, Brandon TA, Entman ML: Cardiac lymph flow in conscious dogs. *Am J Physiol* 1979, 237:H311–317
- Chien KR: Genes and physiology: molecular physiology in genetically engineered animals. *J Clin Invest* 1996, 97:901–909
- James JF, Hewett TE, Robbins J: Cardiac physiology in transgenic mice. *Circ Res* 1998, 82:407–415
- Franz WM, Mueller OJ, Hartong R, Frey N, Katus HA: Transgenic animal models: new avenues in cardiovascular physiology. *J Mol Med* 1997, 75:115–129
- Michael LH, Entman ML, Hartley CJ, Youker KA, Zhu J, Hall SR, Hawkins HK, Berens K, Ballantyne CM: Myocardial ischemia and reperfusion: a murine model. *Am J Physiol* 1995, 269:H2147–2154
- Nossuli TO, Lakshminarayanan V, Baumgarten G, Taffet GE, Ballantyne CM, Michael LH, Entman ML: A chronic mouse model of myocardial ischemia-reperfusion: essential in cytokine studies. *Am J Physiol Heart Circ Physiol* 2000, 278:H1049–1055
- Heymans S, Luttun A, Nuyens D, Theilmeier G, Creemers E, Moons L, Dyspersin GD, Cleutjens JP, Shipley M, Angellilo A, Levi M, Nube O, Baker A, Keshet E, Lupu F, Herbert JM, Smits JF, Shapiro SD, Baes M, Borgers M, Collen D, Daemen MJ, Carmeliet P: Inhibition of plasminogen activators or matrix metalloproteinases prevents cardiac rupture but impairs therapeutic angiogenesis and causes cardiac failure. *Nat Med* 1999, 5:1135–1142
- Orlic D, Kajstura J, Chimenti S, Jakoniuk I, Anderson SM, Li B, Pickel J, McKay R, Nadal-Ginard B, Bodine DM, Leri A, Anversa P: Bone



- marrow cells regenerate infarcted myocardium. *Nature* 2001, 410: 701–705
10. Ducharme A, Frantz S, Aikawa M, Rabkin E, Lindsey M, Rohde LE, Schoen FJ, Kelly RA, Werb Z, Libby P, Lee RT: Targeted deletion of matrix metalloproteinase-9 attenuates left ventricular enlargement and collagen accumulation after experimental myocardial infarction. *J Clin Invest* 2000, 106:55–62
  11. Frangogiannis NG, Lindsey ML, Michael LH, Youker KA, Bressler RB, Mendoza LH, Spengler RN, Smith CW, Entman ML: Resident cardiac mast cells degranulate and release preformed TNF- $\alpha$ , initiating the cytokine cascade in experimental canine myocardial ischemia/reperfusion. *Circulation* 1998, 98:699–710
  12. Frangogiannis NG, Mendoza LH, Lindsey ML, Ballantyne CM, Michael LH, Smith CW, Entman ML: IL-10 is induced in the reperfused myocardium and may modulate the reaction to injury. *J Immunol* 2000, 165:2798–2808
  13. Beckstead JH: A simple technique for preservation of fixation-sensitive antigens in paraffin-embedded tissues. *J Histochem Cytochem* 1994, 42:1127–1134
  14. Gersch C, Dewald O, Zoerlein M, Michael LH, Entman ML, Frangogiannis NG: Mast cells and macrophages in normal C57/BL/6 mice. *Histochem Cell Biol* 2002, 118:41–49
  15. Ismail JA, Poppa V, Kemper LE, Scatena M, Giachelli CM, Coffin JD, Murry CE: Immunohistologic labeling of murine endothelium. *Cardiovasc Pathol* 2003, 12:82–90
  16. Enholm B, Karpanen T, Jeltsch M, Kubo H, Stenback F, Prevo R, Jackson DG, Yla-Herttuala S, Alitalo K: Adenoviral expression of vascular endothelial growth factor-C induces lymphangiogenesis in the skin. *Circ Res* 2001, 88:623–629
  17. Frangogiannis NG, Burns AR, Michael LH, Entman ML: Histochemical and morphological characteristics of canine cardiac mast cells. *Histochem J* 1999, 31:221–229
  18. Frangogiannis NG, Michael LH, Entman ML: Myofibroblasts in reperfused myocardial infarcts express the embryonic form of smooth muscle myosin heavy chain (SMemb). *Cardiovasc Res* 2000, 48:89–100
  19. Hawkins HK, Entman ML, Zhu JY, Youker KA, Berens K, Dore M, Smith CW: Acute inflammatory reaction after myocardial ischemic injury and reperfusion: development and use of a neutrophil-specific antibody. *Am J Pathol* 1996, 148:1957–1969
  20. Ren G, Michael LH, Entman ML, Frangogiannis NG: Morphological characteristics of the microvasculature in healing myocardial infarcts. *J Histochem Cytochem* 2002, 50:71–79
  21. Zeng L, Takeya M, Ling X, Nagasaki A, Takahashi K: Interspecies reactivities of anti-human macrophage monoclonal antibodies to various animal species. *J Histochem Cytochem* 1996, 44:845–853
  22. Frangogiannis NG, Mendoza LH, Ren G, Akrivakis S, Jackson PL, Michael LH, Smith CW, Entman ML: MCSF expression is induced in healing myocardial infarcts and may regulate monocyte and endothelial cell phenotype. *Am J Physiol Heart Circ Physiol* 2003, 285: H483–492
  23. Frangogiannis NG, Perrard JL, Mendoza LH, Burns AR, Lindsey ML, Ballantyne CM, Michael LH, Smith CW, Entman ML: Stem cell factor induction is associated with mast cell accumulation after canine myocardial ischemia and reperfusion. *Circulation* 1998, 98:687–698
  24. Frangogiannis NG, Youker KA, Rossen RD, Gwechenberger M, Lindsey MH, Mendoza LH, Michael LH, Ballantyne CM, Smith CW, Entman ML: Cytokines and the microcirculation in ischemia and reperfusion. *J Mol Cell Cardiol* 1998, 30:2567–2576
  25. Jones SP, Lefer DJ: Using gene-targeted mice to investigate the pathophysiology of myocardial reperfusion injury. *Basic Res Cardiol* 2000, 95:499–502
  26. Frangogiannis NG, Smith CW, Entman ML: The inflammatory response in myocardial infarction. *Cardiovasc Res* 2002, 53:31–47
  27. Richard V, Murry CE, Reimer KA: Healing of myocardial infarcts in dogs: effects of late reperfusion. *Circulation* 199, 92:1891–1901
  28. Kukielka GL, Hawkins HK, Michael L, Manning AM, Youker K, Lane C, Entman ML, Smith CW, Anderson DC: Regulation of intercellular adhesion molecule-1 (ICAM-1) in ischemic and reperfused canine myocardium. *J Clin Invest* 1993, 92:1504–1516
  29. Sun B, Fan H, Honda T, Fujimaki R, Lafond-Walker A, Masui Y, Lowenstein CJ, Becker LC: Activation of NF  $\kappa$ B and expression of ICAM-1 in ischemic-reperfused canine myocardium. *J Mol Cell Cardiol* 2001, 33:109–119
  30. Zhao ZQ, Lefer DJ, Sato H, Hart KK, Jefforda PR, Vinten-Johansen J: Monoclonal antibody to ICAM-1 preserves postischemic blood flow and reduces infarct size after ischemia-reperfusion in rabbit. *J Leukoc Biol* 1997, 62:292–300
  31. Gwechenberger M, Mendoza LH, Youker KA, Frangogiannis NG, Smith CW, Michael LH, Entman ML: Cardiac myocytes produce interleukin-6 in culture and in viable border zone of reperfused infarctions. *Circulation* 1999, 99:546–551
  32. Ivey CL, Williams FM, Collins PD, Jose PJ, Williams TJ: Neutrophil chemoattractants generated in two phases during reperfusion of ischemic myocardium in the rabbit: evidence for a role for C5a and interleukin-8. *J Clin Invest* 1995, 95:2720–2728
  33. Kukielka GL, Smith CW, LaRosa GJ, Manning AM, Mendoza LH, Daly TJ, Hughes BJ, Youker KA, Hawkins HK, Michael LH, Rot A, Entman ML: Interleukin-8 gene induction in the myocardium after ischemia and reperfusion in vivo. *J Clin Invest* 1995, 95:89–103
  34. Kumar AG, Ballantyne CM, Michael LH, Kukielka GL, Youker KA, Lindsey ML, Hawkins HK, Birdsall HH, MacKay CR, LaRosa GJ, Rossen RD, Smith CW, Entman ML: Induction of monocyte chemoattractant protein-1 in the small veins of the ischemic and reperfused canine myocardium. *Circulation* 1997, 95:693–700
  35. Frangogiannis NG, Mendoza LH, Lewallen M, Michael LH, Smith CW, Entman ML: Induction and suppression of interferon-inducible protein 10 in reperfused myocardial infarcts may regulate angiogenesis. *FASEB J* 2001, 15:1428–1430
  36. Yang Z, Zingarelli B, Szabo C: Crucial role of endogenous interleukin-10 production in myocardial ischemia/reperfusion injury. *Circulation* 2000, 101:1019–1026
  37. Shah M, Foreman DM, Ferguson MW: Neutralising antibody to TGF- $\beta$ 1, 2 reduces cutaneous scarring in adult rodents. *J Cell Sci* 1994, 107 (Pt 5):1137–1157
  38. Shah M, Foreman DM, Ferguson MW: Neutralisation of TGF- $\beta$ 1 and TGF- $\beta$ 2 or exogenous addition of TGF- $\beta$ 3 to cutaneous rat wounds reduces scarring. *J Cell Sci* 1995, 108(Pt 3):985–1002
  39. Sasayama S, Okada M, Matsumori A: Chemokines and cardiovascular diseases. *Cardiovasc Res* 2000, 45:267–269
  40. Gabbiani G, Le Lous M, Bailey AJ, Bazin S, Delaunay A: Collagen and myofibroblasts of granulation tissue: a chemical, ultrastructural and immunologic study. *Virchows Arch B Cell Pathol* 1976, 21:133–145
  41. Willems IE, Havenith MG, De Mey JG, Daemen MJ: The  $\alpha$ -smooth muscle actin-positive cells in healing human myocardial scars. *Am J Pathol* 1994, 145:868–875
  42. Cleutjens JP, Kandala JC, Guarda E, Guntaka RV, Weber KT: Regulation of collagen degradation in the rat myocardium after infarction. *J Mol Cell Cardiol* 1995, 27:1281–1292
  43. Desmouliere A, Geinoz A, Gabbiani F, Gabbiani G: Transforming growth factor- $\beta$  1 induces  $\alpha$ -smooth muscle actin expression in granulation tissue myofibroblasts and in quiescent and growing cultured fibroblasts. *J Cell Biol* 1993, 122:103–111
  44. Modi WS, Yoshimura T: Isolation of novel GRO genes and a phylogenetic analysis of the CXC chemokine subfamily in mammals. *Mol Biol Evol* 1999, 16:180–193
  45. Birmingham DJ, Rovin BH, Yu CY, Hebert LA: Of mice and men: the relevance of the mouse to the study of human SLE. *Immunol Res* 2001, 24:211–224
  46. Yao L, Setiadi H, Xia L, Laszik Z, Taylor FB, McEver RP: Divergent inducible expression of P-selectin and E-selectin in mice and primates. *Blood* 1999, 94:3820–3828
  47. Barrett KE, Metcalfe DD: Mast cell heterogeneity: evidence and implications. *J Clin Immunol* 1984, 4:253–261
  48. Jugdutt BI, Joljart MJ, Khan MI: Rate of collagen deposition during healing and ventricular remodeling after myocardial infarction in rat and dog models. *Circulation* 1996, 94:94–101